Mechanical properties of epidermal cells of whole living roots of *Arabidopsis thaliana*: An atomic force microscopy study

Anwesha N. Fernandes,[1,*] Xinyong Chen,[2] Colin A. Scotchford,[3] James Walker,[3] Darren M. Wells,[1] Clive J. Roberts,[2] and Nicola M. Everitt[3]

[1]*Centre for Plant Integrative Biology, School of Biosciences, University of Nottingham, England LE12 5RD*
[2]*Laboratory of Biophysics and Surface Analysis, School of Pharmacy, University of Nottingham, England NG7 2RD*
[3]*Division of Materials, Mechanics and Structures, Faculty of Engineering, University of Nottingham, England, NG7 2RD*

(Received 5 January 2011; revised manuscript received 10 August 2011; published 21 February 2012)

The knowledge of mechanical properties of root cell walls is vital to understand how these properties interact with relevant genetic and physiological processes to bring about growth. Expansion of cell walls is an essential component of growth, and the regulation of cell wall expansion is one of the ways in which the mechanics of growth is controlled, managed and directed. In this study, the inherent surface mechanical properties of living *Arabidopsis thaliana* whole-root epidermal cells were studied at the nanoscale using the technique of atomic force microscopy (AFM). A novel methodology was successfully developed to adapt AFM to live plant roots. Force-Indentation (F-I) experiments were conducted to investigate the mechanical properties along the length of the root. F-I curves for epidermal cells of roots were also generated by varying turgor pressure. The F-I curves displayed a variety of features due to the heterogeneity of the surface. Hysteresis is observed. Application of conventional models to living biological systems such as cell walls in nanometer regimes tends to increase error margins to a large extent. Hence information from the F-I curves were used in a preliminary semiquantitative analysis to infer material properties and calculate two parameters. The work done in the loading and unloading phases (hysteresis) of the force measurements were determined separately and were expressed in terms of "Index of Plasticity" (η), which characterized the elasticity properties of roots as a viscoelastic response. Scaling approaches were used to find the ratio of hardness to reduced modulus ($\frac{H}{E^*}$).

DOI: 10.1103/PhysRevE.85.021916 PACS number(s): 87.19.R−, 87.64.−t

I. INTRODUCTION

The root is one of the main life sustaining organs of a plant system. It normally supplies nutrients to the system besides providing a mechanically robust base that anchors and supports the shoot system. Root research has been impeded by methodological and technical difficulties as they grow in soil [1] and are inaccessible to traditional experimental analysis. Studies of the mechanical properties of cells and other biological tissues at high resolution is instrumental to understanding how mechanical interactions affect functions. Biomechanics is a research area complementary to molecular and cell biological methods used to study root systems and is indispensable in the quest to obtain a complete picture of the mechanisms of growth and development, providing information to fill the gaps in our knowledge [2]. The root cell wall is a complex polymeric sheath, consisting of a network of cellulose microfibrils interspersed with a polysaccharide matrix and is mechanically anisotropic. The cell wall is a major determinant of cell mechanical properties and cell shape. It allows cells to attain high turgor pressure (internal hydrostatic pressure) due to which the wall experiences a high tensile stress.

Cell growth is a mechanical process that balances internal and external stresses with the compliance to allow expansion. Plant cells are compared to "hydraulic machines" due to the similar concept of balanced counterforce between the primary wall stresses and the turgor pressure [3]. Knowledge of cell mechanics is vital for understanding plant wall functioning and consequently growth.

Figure 1(a) shows the morphology of a root [4]. Roots can be categorized into four distinct zones lengthwise [Fig. 1(b)], namely, the root tip meristem, the accelerating elongation zone, the decelerating elongation zone and the mature zone [5]. It is hypothesized that root growth is accompanied by changes in cell wall properties of cells within these regions. Cell expansion occurs within a defined region close to the root apex termed the elongation zone. So the elongation growth of a root is a consequence of the expansion of the individual cells in the growing zone of the tissue [6]. Growth rate is regulated by the combined activity of two related processes, expansion and cell production [7]. Cell expansion is dependent on the mechanics of cell wall dynamics. Cell wall expansion is driven by turgor pressure inside the cell, but as turgor is constant (D. M. Wells, unpublished results), the expansion is influenced by the mechanical behavior of the cell wall itself. Loosening of structure of the cell wall is necessary in this case, besides the synthesis of new material and its subsequent integration in the cell wall [8]. One method that enables qualitative and quantitative analysis of mechanical properties is atomic force microscopy (AFM), and it is possible to adapt this method to permit measurements of mechanical properties of living cells in conditions close to relevant physiological environments [9]. In this study we use AFM to investigate properties of whole epidermal cells, which are the cells that form the outermost layer of the root. These epidermal cells are studied *in situ* in a living root and are influenced by the inherent multicellular properties of the root, which is an improvement over studies performed on isolated living cells.

*anwesha.fernandes@nottingham.ac.uk

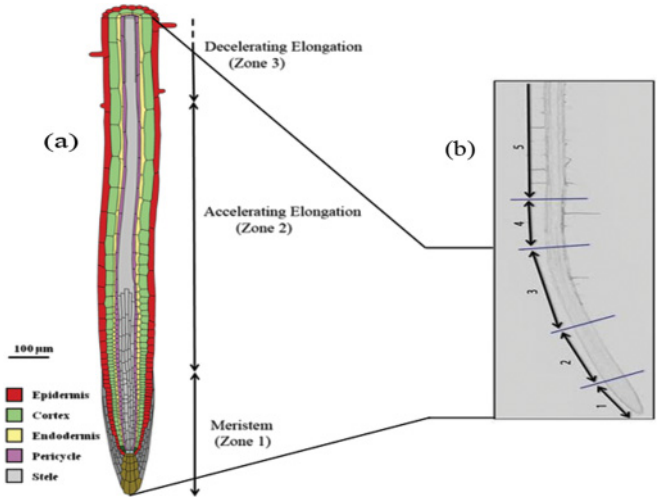

FIG. 1. (Color online) (a) Schematic structure of a root growth region (adapted from Ref. [4]). (b) The different designated zones in the root: (1) meristem (∼350 μm); (2) accelerating elongation (∼900 μm); (3) decelerating elongation (∼1.2 mm); (4) mature (reference) (∼500 μm); (5) rest of the root-lateral root emergence zone (∼2.5 cm) [5].

A. Atomic force microscopy

AFM is not only a tool to image topography of solid surfaces but can also be used to generate force-versus-distance curves from points of contact between the AFM probe and a surface. These curves can provide valuable information on local material properties such as elasticity, hardness, adhesion, and surface charge densities. The measurement of force curves in different fields of research such as surface science, materials engineering, and biology helped unravel interesting results [10]. This particular type of microscopy has opened new exciting avenues in biology and biophysics for probing nanomechanical properties [11]. In a force measurement, generally a sharp tip is mounted on a cantilever spring. This is brought toward and away from the sample in the normal direction. Vertical position of the tip and deflection of the cantilever are recorded and then converted into a force-versus distance curve [12]. The movement of the tip-cantilever assembly is achieved by applying a varied voltage to a piezoelectric translator, onto which the cantilever is attached. The deflection of the cantilever, which measures the tip-sample interactive forces, is detected by a laser and a split photodiode system.

Force spectroscopy generates a force-distance curve for a single location on the sample. This is a plot of the magnitude of the force acting between the tip and the sample versus the position of the scanner in the direction normal to the substrate. Force-distance curves convey a lot of information about the sample's mechanical properties. Points of discontinuity, the slopes of approach and retraction curves, as well as any observed hysteresis all convey information about surface characteristics. In addition, viscoelastic properties can be determined from these plots.

An array of force-distance curves are usually collected at separate sites over an area of the sample surface to study effects of surface heterogeneity [13]. Capella *et al*. record how AFM force-distance curves have become a fundamental tool in several fields of research and how they are important for studying surface interactions [12]. For biological materials, the AFM force curves have been used to examine mechanical properties of bones, bacteria, epithelial cells, and other materials [14]. AFM is an appropriate tool to help study wall properties in the different zones of the root, as seen in Fig. 1(b). We have attempted to use this technique to qualitatively study the elasticity properties of root cells using the force-distance plots generated by AFM and to quantify the hardness to reduced elastic modulus ratio for the root epidermal cells.

B. Quantifying hysteresis and energy dissipation

An indentation loading curve is the relationship between load, F, and displacement, z, that can be continuously measured during an indentation experiment. In pure elastic deformations (indentation in elastic solids), unloading curves would retrace loading curves, and there will be no hysteresis between them [13]. In contrast, curves for indentation in elastic-plastic (viscoelastic) solids that display hysteresis have attracted much study. Both loading and unloading curves are recorded for data analysis as seen in Fig. 2. The data obtained from the loading and unloading curves provide information regarding the elastic, viscoelastic and plastic behavior [15].

By integrating the loading and unloading curves, the work of indentation can be readily obtained. Specifically the area under the loading curve is the total work done, W_{tot}; the area under the unloading curve is the reversible work, W_u; and the area enclosed by the loading and unloading curve is irreversible work of indentation, W_{hys} [16]. So the total work done is

$$W_{\text{tot}} = W_u + W_{\text{hys}}. \tag{1}$$

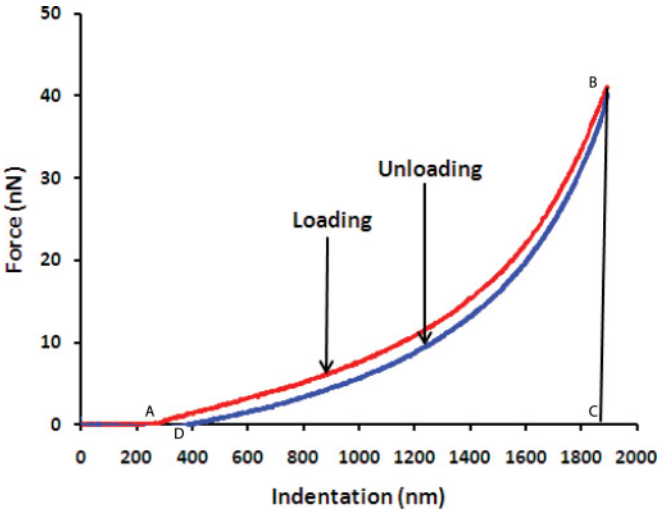

FIG. 2. (Color online) An example of a single loading-unloading indentation curve from which the index of plasticity can be determined. This curve was generated at a distance of 0.5 mm from the root tip in water. ABC is area under the loading curve, and DBC is area under the unloading curve.

The plasticity index (η) of a solid body is a parameter that characterizes the relative plastic or elastic behavior of the material when it undergoes external stresses and strains [17]. This is a relatively simple and nondestructive means of assessing mechanical properties of solids. Lekka *et al.* [9] have applied this methodology to study the mechanical states of cell cytoskeleton of human skin fibroblast and melanoma cell lines. We have used this method to quantify the elastic properties of the epidermal cell wall in living plant roots. During AFM experiments, hysteresis between the loading and unloading curves is observed, indicating the dissipation of energy during the indentation measurement. Hence, studies were focused on quantification of such hysteresis by introduction of η [9,17]. From indentation measurements, η, can be determined easily from the ratio between areas under the loading and unloading curves (work done) [9]:

$$\eta = 1 - \frac{A_2}{A_1}, \tag{2}$$

where A_1 and A_2 are areas under loading and unloading curves.

The *index of plasticity* encompasses the range between $\eta = 0$, when $A_2 = A_1$, the loading and unloading curves overlap (fully elastic behavior), and $\eta = 1$ when $A_2 = 0$ (fully plastic), while the intermediate values $0 < \eta < 1$ indicate mixed viscoelastic-plastic properties [9].

Writing Eq. (2) in terms of Eq. (1) gives

$$\eta = \frac{W_{\text{hys}}}{W_{\text{tot}}}. \tag{3}$$

C. Application of scaling techniques to find $\frac{H}{E^*}$

Attempts to measure the stiffness properties of living cells are challenging. It is not easy to preserve the viability of the cells while executing the experiment and to indent the cells without inducing damage. Plant root living cells, like most biological materials, are anisotropic, nonhomogenous in nature, and have characteristic shapes due to the presence of turgor pressure. They are not purely elastic materials, but exhibit hysteresis and other effects indicative of viscoelasticity [18].

The complexity of certain biological structures like the root cell walls poses a major challenge in fitting the recorded data to an appropriate mathematical model, which is necessary to yield absolute values for the elastic modulus. Many factors external to the biological object must be taken into account, including the geometry of the cantilever tip and its contact area with the sample. Many AFM mechanical measurements on living cells rely on nanoindentation approaches to extract relevant mechanical parameters from measured force-displacement curves [19].

Among the analysis methodologies from nanoindenation techniques used in AFM studies, the most commonly used is an adaptation of the Oliver-Pharr model based on relationships developed by Sneddon. The Oliver-Pharr models have two key observations, namely, the slope of the unloading curve changes constantly due to constantly changing contact area; and, second, if the unloading curve can be fitted by a power expression, then a derivative $\frac{dF}{dh}$ applied at the maximum loading point should yield information about the load at the contact point. This derivative is termed stiffness [20]. Sneddon's solution [Eq. (4)] for the indentation of an elastic half space by a rigid axisymmetric indenter is basically the cornerstone for determining elastic moduli from nanoindentation load-displacement data:

$$E^* = \frac{E}{1-\nu^2} = \frac{\sqrt{\pi}}{2}\frac{S}{\sqrt{A}}, \tag{4}$$

where E^* is the effective reduced elastic modulus defined in terms of Young's modulus E and Poisson's ratio ν, S is the contact stiffness, and A is the projected contact area [21]. This work was incorporated by Oliver and Pharr in their model to give the unloading slope equation as seen in Eq. (5):

$$\frac{dF}{dh} = \frac{2}{\sqrt{\pi}}E^*\sqrt{A}, \tag{5}$$

where $\frac{dF}{dh}$ is the initial unloading slope and A is the projected contact area evaluated at $h = h_m$ and E^* is the reduced elastic modulus. The most commonly used hardness definition in the protocols for indentation measurements is given in Eq. (6) [16]:

$$H = \frac{F}{A_c}, \tag{6}$$

where A_c is the projected contact area under load F.

The accuracy with which the elastic moduli can be measured depends on how well Sneddon's solution describes real material behavior. Oliver and Pharr have further modified their equations to adapt for several cases [22], and refinements of models are constantly taking place.

Gindl *et al.* have performed indentation tests on wood cell walls and have used the theory of nanoindentation [23] for analysis. It does not consider the effects of anisotropy found in wood cell walls in a three-dimensional stress state. So the nanoindentation of wood cell walls using this theory is not perfectly suitable for the direct determination of the absolute value of the longitudinal elastic modulus of wood cell walls, but it is nevertheless a suitable technique for comparisons of mechanical properties of wood and plant fiber cell walls at a small scale [23]. If we extend this methodology, which uses isotropic theory, to anisotropic living plant roots, it would not be ideally appropriate for extracting absolute values. Furthermore, this is a study looking at inherent mechanical properties of live root epidermal cells along the length of the root rather than aiming to extract an absolute value for elastic modulus. Characterizing hardness of cell walls as a property is not very easy and straightforward to interpret due to matrix influence, heterogeneous phase composition, and mechanical anisotropy [33,34]. Instead of directly deriving an absolute elastic modulus from the Oliver-Pharr model or other adapted models, we used the ratio of relative hardness to reduced modulus, $\frac{H}{E^*}$ using Eqs. (4) and (6), respectively. Living root epidermal cells are unique pressurized systems and need exclusive models to describe them. Hence using the ratio approach is a cautious way to describe this system as it can incorporate relevant parameters that still need to be considered and eliminate errors arising from spring constant values of the cantilevers.

In the current study we have employed AFM to develop and demonstrate a novel way of studying live multicellular whole roots of *Arabidopsis thaliana* and obtain information on

relevant mechanical properties. The advantage of this method is that it allows direct mechanical contact between the probe and sample surface and hence can be used to quantify the surface properties of the material. This technique can be used to map the stiffness properties of the root along the length, more specifically, the inherent surface mechanical properties of root cells along the length of the root. Information from resultant F-I plots can be used to extract the index of plasticity (η), which gives a measure of material elasticity.

A value for the ratio of hardness to reduced modulus $\frac{H}{E^*}$ can also be inferred. Hence two different parameters can be quantified. The turgor pressure was also varied using sorbitol as a hyperosmotic liquid medium in order to establish whether the AFM experiments reflect cell wall properties of the epidermal cell wall or the influence of turgor pressure.

II. MATERIALS AND EXPERIMENTAL METHODS

A. Instrumentation: Atomic Force Microscope

The instrument used for the experiments was a D3000 (Veeco, Santa Barbara, CA) with a liquid cell. All measurements were conducted using triangular SiN_4 cantilever tips (NP-Veeco) and were done at room temperature. The spring constant of the cantilevers was 0.58 N/m. Force curves were recorded with a velocity of 0.5 μm/s. Roots of *Arabidopsis thaliana* ecotype Columbia 0 were studied at approximately 7 days old. An online optical microscope was used to align the AFM tip at the appropriate points on the root surface. Plant roots were tested from the root tip columella through the meristem to the elongation zone to see if it were possible to identify discernible variation in mechanical properties using AFM. Each living sample was tested in water and sorbitol, one after the other in a single experiment. Force-Indentation data sets were generated at a single point along the root in each case. The protocol we selected was to record single measurements at different points along the length of the root as taking several measurements at a single point on the root surface has the potential to modify or even damage the living root tissue. A total of 15 experiments were conducted. Some data sets did not generate force curves at necessary points along the length of the root and were not included. This was due to the practical difficulties of working with whole living tissue. Analysis for five complete data sets are shown here.

Figure 3 shows an example of force-versus-displacement z curve for a living root.

The force F is obtained by multiplying the deflection of the cantilever with its spring constant $k_c = 0.58$ N/m: $F = k_c Z_c$ [26]. The force-displacement curve in Fig. 3 can be converted into a force-indentation curve, as seen in Figs. 2 and 5. To calculate indentation, a reference hard glass surface is used. On a hard surface, when a force measurement is conducted, there is no indentation into the surface. Hence, after the probe is in contact with the surface, any change in the z scanner displacement equals the change in cantilever deflection. On a soft surface, to reach the same cantilever deflection, the z scanner needs to displace a larger amount because of the indentation into the sample surface. The difference between the hard and soft surface gives the indentation into the sample surface.

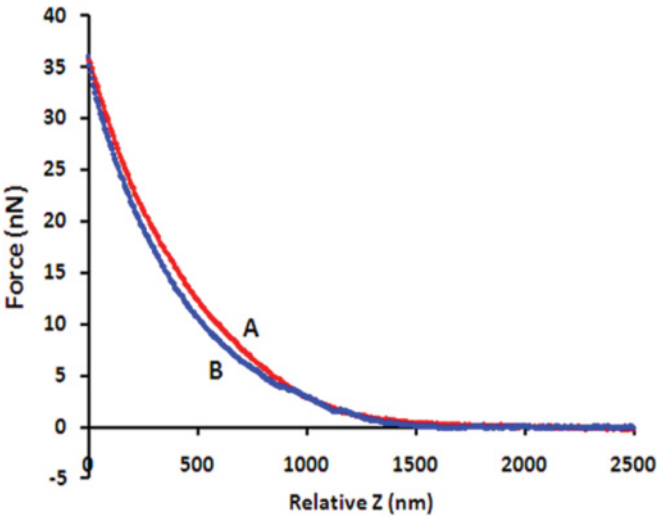

FIG. 3. (Color online) An example of force-versus-displacement curve on the sample surface. A is the loading curve, and B is the unloading curve.

One of the main limitations for the application of AFM to the study of biologically relevant samples is the sample preparation. While the study of more rigid materials can be carried out in high resolution with no damage to the samples, softer materials can be deformed or dragged away by the tip. Similarly, studies in aqueous solution can give rise to different problems such as inadequate sample attachment to substrates. There is no universal solution to deal with these problems, making it necessary to develop a specific method for each type of system. For the study of biological samples, it is important to find a method that binds the sample to the substrate, so that the binding is not only strong enough to avoid the dragging by the tip but simultaneously does not cause structural alteration in the sample. As in other types of microscopy methods, the biological sample has to be deposited and in this case firmly attached onto a solid substrate [10]. The most common substrates for AFM studies are glass and mica. We have used glass as the substrate throughout. An additional requirement in cases where samples are to be kept alive is that the relevant environments are not toxic.

III. DEVELOPMENT OF THE TECHNIQUE

AFM experiments have not been attempted previously on living roots to the best of our knowledge. Experiments involving force measurements based on fixed cells or biological materials are plausible and have been conducted [10,27]. The main challenges in developing this experimental technique is keeping the root alive and obtaining reproducible data sets. The experiment had to be done in water in order to keep the root alive. So a wet cell with compatible AFM tips had to be used, a unique ability of AFM that can be used for such nanoscale measurements. The root had to be kept attached to the surface of the substrate in water for a considerable amount of time, so several different attachment methods, including adhesives, were tested for compatibility. The adhesive had to have properties that included quick drying traits and held the root attached to the substrate in water while keeping it alive and not dissipating into the surrounding medium or reacting

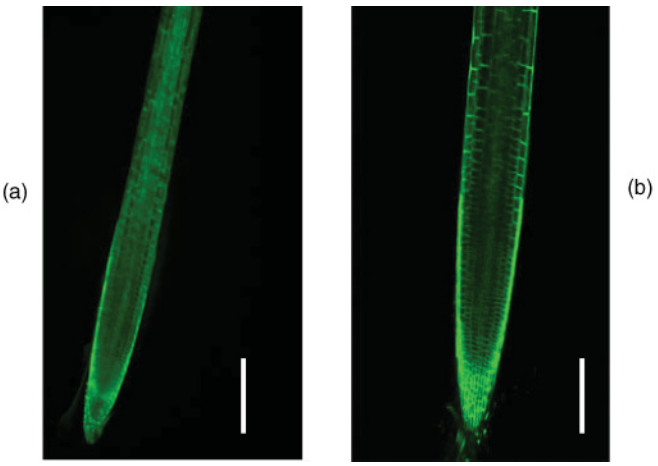

FIG. 4. (Color online) (a) Confocal image of a root in experimental conditions (for AFM) on a glass substrate attached with a fixative. (b) Confocal image of a root in normal conditions (scale bar: 100 μm).

with it. We also looked at different surface compatibilities; this was largely due to the need to keep the root alive in water with minimum complexity. It was necessary to position the root flat and straight on the substrate in order to avoid any kinks that would bring about mechanical stress on parts of the root, which would have adverse effects on the system. Besides, problems with some roots being nonideal candidates due to biological variabilities meant that they had to be discarded after being prepared for the experiment. Confocal microscopy (Nikon Eclipse TiU confocal microscope) was undertaken to establish that the roots remained alive under the experimental conditions developed, for the duration of a typical AFM experiment as seen in Fig. 4. The root morphologies are observed to be similar in both the cases in Fig. 4 and establish that the roots kept under AFM experimental conditions are not adversely affected. Time-of-flight Secondary Ion Mass Spectroscopy (ToF-SIMS) analysis showed no evidence of the fixative (Evostick glue) being released into the aqueous media [28], suggesting that little or no diffusion occurred into the aqueous medium. Therefore, information derived from both the techniques suggests that the roots are alive while the experiments are conducted.

IV. RESULTS AND DISCUSSION

A. Force-indentation experiments

Force-indentation (F-I) experiments were performed on living roots of *Arabidopsis thaliana*. Roots were tested in water and sorbitol (1 M) consecutively in individual experiments to see if there was any difference in perceived cell wall properties. A selection of force indentation plots of a single root in the two media is seen in Fig. 5. It is obvious that the curves have different shapes, which signify the heterogeneity of the surface. Some plots exhibit very pronounced changes in gradients, which indicate the presence of two different phases, namely, an initial rapid softer phase that progressively stiffens as the indentation deepens. F-I curves were generally observed to be comparatively stiff near the tip of the root meristem compared to further along the length of the root. This could be due to the sheath-like protective root cap, which is present at the root tip. The varied profiles of the F-I curves for root reflect the cell wall complex architecture. Hysteresis due to energy dissipation was observed frequently.

There was no clear distinguishable difference observed between the water and sorbitol F-I curves as seen in Fig. 5. It is normally assumed that stiffer samples will deform less than a soft one. Consequently, stiffer areas will offer high resistance to the vertical oscillations of the cantilever thereby causing its greater bending [29]. It is also observed that flaccid tissue undergoes larger deformation than cells at normal turgor pressure at similar stress loads. Turgor pressure in roots usually changes in the presence of hyperosmotic stress inducers [30] like sorbitol or mannitol [31]. So when a root loses water, the turgor pressure decreases, which would bring about a decrease in the overall stiffness of the root, and thereby a striking consistent difference should be noticed in the F-I

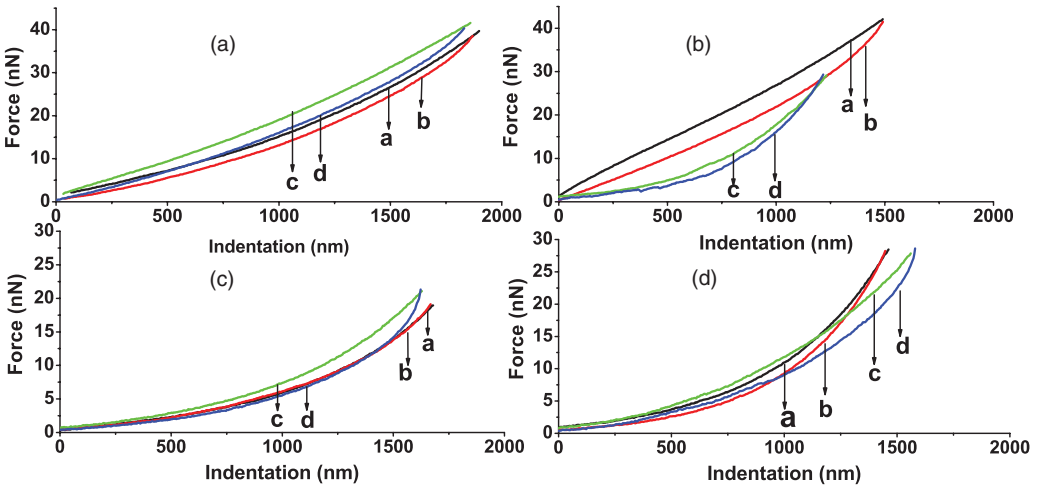

FIG. 5. (Color online) A selected range of force-indentation (F-I) curves along the length of the root. (a) F-I curves at 0.2 mm distance from the root tip (meristem zone). (b) F-I curves at 0.6 mm distance from the root tip (accelerating elongation zone). (c) F-I curves at 1 mm distance from the root tip (decelerating elongation zone). (d) F-I curves at 1.5 mm distance from the root tip (mature zone). In each panel a and b are loading and unloading curves in water, respectively, and c and d are loading and unloading curves in sorbitol, respectively.

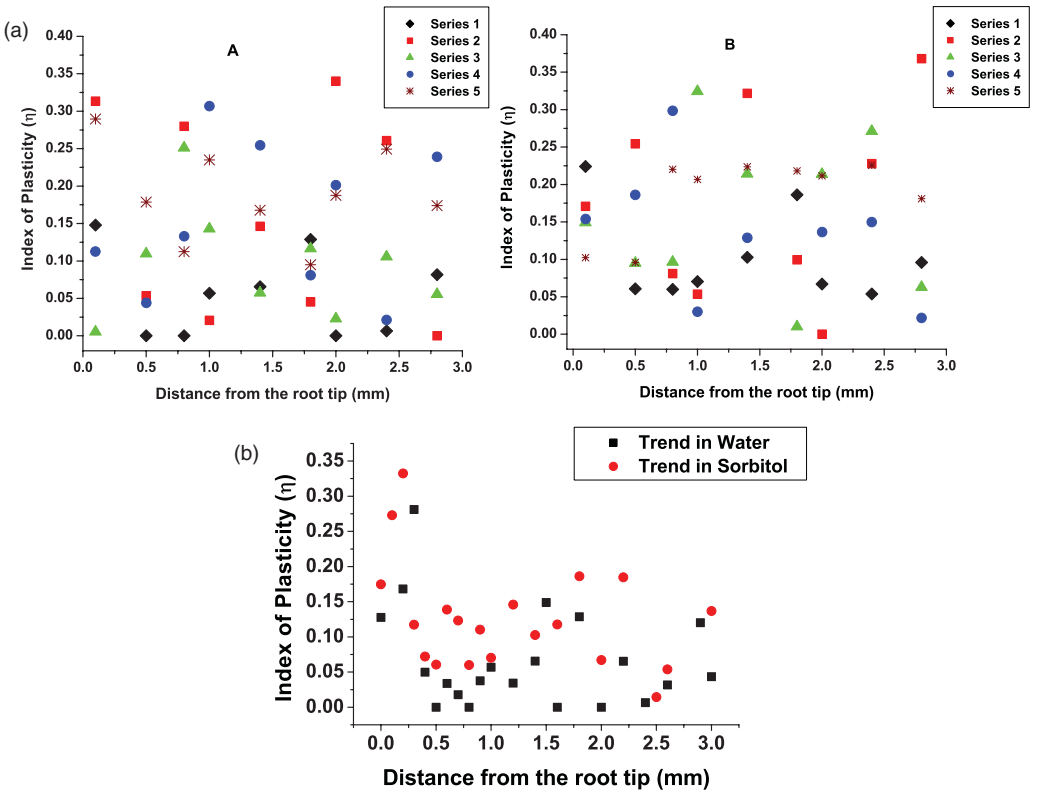

FIG. 6. (Color online) The index of plasticity η values for living root samples in water and sorbitol. The index of plasticity η plots are observed to be in a similar reproducible range over a sample of individual sets within the remits of biological variability. (a) Index of plasticity η values range in five different sets of root samples where experiments in A-water and B-sorbitol on each root were typically performed one after the other. (b) A single graph of the index of plasticity η of root from the root tip in both water and sorbitol.

curves in the presence of sorbitol compared to that of water. Figure 5(b) shows a difference, though such behavior is not observed consistently in all data sets. One of the reasons for this difference not being registered could be that conducting an experiment in force mode in the nanometer regime could render turgor pressure influence to be negligible. Another major plausible error is due to the AFM tip dynamics and is a commonly acknowledged problem in the field of AFM modeling [12]. In the current experimental conditions, it is possible that we cannot detect subtle differences using sharp conical tips, especially the comparative difference between water and sorbitol environments as the tip indents a small surface volume. F-I experiments by using spheres attached to tips are being considered as it would encompass a larger surface volume. In addition, living materials have a very varied stimulus response as it is a dynamic system that adapts to its mechanochemical environment [32], and this has to be taken into consideration as a source of viable biological error. Since the AFM experiments conducted in the presence of sorbitol showed no clear consistent difference compared to those in water, our observations suggest that the results are independent of the influence of turgor pressure, and thereby the observed properties are derived from inherent local cell wall properties within the limitations of the technique.

B. Index of plasticity

Figure 6(a) shows a selection of data from a series of experiments used to calculate the index of plasticity (η) in several samples. These plots shows similarity in range of the material over a number of individual data sets. Figure 6(b) shows the index of plasticity (η) along the length of a single root in water and sorbitol for clarity purposes. It suggests that there is a deviation from elastic behavior, which can be termed viscoelastic. It can be also said that the scatter in η implies the heterogeneity of cell surface, pointing out locations of large or smaller energy dissipation. Here (η) for living plant cell walls is observed to be between 0 and 0.4 as seen in Fig. 6, which indicates that the observed viscoelasticity (intermediate values) is more viscoelastic-elastic in nature than viscoplastic-plastic. It has also been largely observed that the values of the index of plasticity are generally higher at the tip of the root compared to further up along the length of the root, and this could be due to the presence of the root cap.

Biological variability is an inherent problem while doing experiments on plant samples, though we have successfully demonstrated an excellent level of reproducibility in the range of values for η as seen in Fig. 6(a). In addition, we have to consider the aspect that we were working with a live sample and were not recording the physiological responses to the mechanical stimuli.

C. Determination of $\frac{H}{E^*}$ for living roots

We have attempted to quantify a ratio of hardness to reduced elastic modulus ($\frac{H}{E^*}$) for living root epidermal cells. This ratio is of significant interest to both tribology and fracture

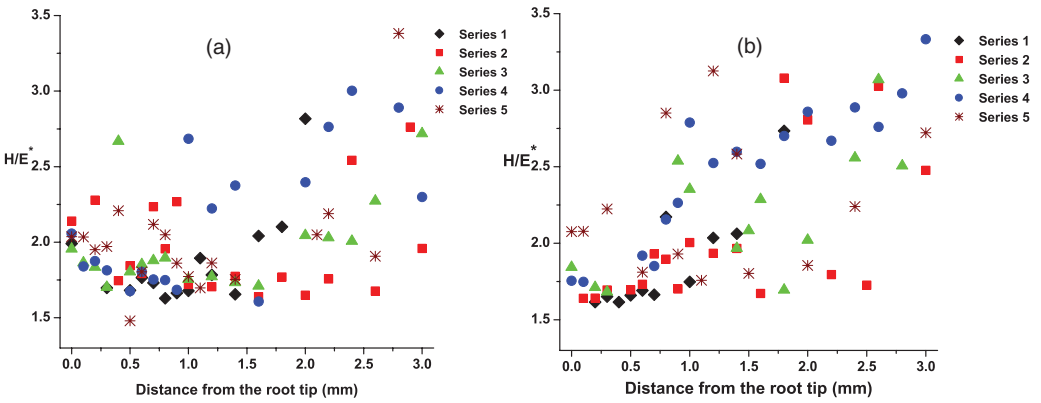

FIG. 7. (Color online) The ratio of hardness to reduced modulus $\frac{H}{E^*}$ values in five different sets of roots samples where experiments in (a) water and (b) sorbitol on each living root were performed one after the other.

mechanics, and we have attempted to apply it as a first approximation to an anisotropic, viscoelastic, living material like whole root cells for quantification. The unloading slope [Eq. (5)] was applied to derive the value for the reduced Young's modulus, E^*, for a live root, and hardness was calculated using Eq. (6). The $\frac{H}{E^*}$ dynamics along the length of the root were plotted as seen in Fig. 7. The graphical scatter variations are similar in nature to the index of plasticity curves seen in Fig, 6. These data sets also show that there is no clear difference in the properties in water and sorbitol media. The values for $\frac{H}{E^*}$ are in the range of 1.5–3.25 as seen in Fig. 7. There is not much evidence in literature for $(\frac{H}{E^*})$ studies with regards to soft living plant-based materials. However, here we have shown that the hardness to reduced modulus ratio $\frac{H}{E^*}$ can be used as a parameter that gives reproducible results within the experimental scatter for a series of experiments.

V. CONCLUSIONS

Plant root cell walls play an important part in cell expansive growth and providing support. Studying the mechanical properties of the cell wall can provide insight into the biophysical control of root elongation. We have explored the stiffness properties of epidermal cells of living root using atomic force microscopy (AFM). A new methodology for AFM on live plant roots has been successfully developed. The method addressed the challenges of keeping the sample alive and robustly anchored to a suitable substrate and had to be performed in wet conditions. AFM local F-I plots have been recorded from the root tip until 2 mm along the length of the root, that is, from the root tip meristem to approximately the decelerating elongation zone. The curves showed a mixture of hysteresis and elastic responses, which were a reflection of the heterogeneity of the root surface. There were no clear differences observed in the mechanical properties along the length of the root. Turgor pressure was altered with the usage of sorbitol as a hyperosmotic medium in an attempt to determine whether cell wall mechanical properties were affected by turgor pressure. No discernible difference could be seen in the curves generated for each media indicating that, within experimental scatter, we can extract cell wall mechanical properties independent of the turgor pressure of the system. As a living root cell wall is a singular system, a model for a pressurized system is currently being developed. The index of plasticity, (η), has been calculated for roots and shows that the epidermal cells are viscoelastic in nature. A ratio of hardness to reduced modulus $(\frac{H}{E^*})$ was calculated. Thus using scaling approaches, good results were observed for a biological system like plant roots that exemplifies that scaling and dimensional analysis can be used in quantifying mechanical properties to a reasonable degree in similar nonuniform systems. Further experimental work involving studies of loading force effects on the hardness properties of deeper tissues of the root, ramp rate effects on the relaxation of cell wall deformation, and general time-based evolution of root cell mechanical properties are planned.

ACKNOWLEDGMENTS

The authors would like to thank Dr. D. Scurr, School of Pharmacy, University of Nottingham, for ToF-SIMS measurements. The authors also acknowledge the Bridging the Gap award for an interdisciplinary summer project (University of Nottingham) that financed the pilot project on this study. CPIB is a center for Integrative Systems Biology funded by the BBSRC and the EPSRC. The authors would also like to thank anonymous referees for constructive comments.

[1] Y. Waisel, A. Eshel, and U. Kafkafi, *Plant Roots: The Hidden Half* (Marcel Dekker, New York, 2002).
[2] S. Kerstens and J. P. Verbelen, J. Struct. Biol. **144**, 262 (2003).
[3] A. Geitmann and J. K. E. Ortega, Trends Plant Sci. **14**, 467 (2009).
[4] P. N. Benfey, M. Bennett, and J. Schiefelbein,Plant J. **61**, 992 (2010).
[5] B. De Rybel, V. Vassileva, B. Parizot, M. Demeulenaere1, W. Grunewald, D. Audenaert, J. Van Campenhout, P. Overvoorde, L. Jansen, S. Vanneste, B. Möller, M. Wilson, T. Holman, G. Van

Isterdael, G. Brunoud, M Vuylsteke, T. Vernoux, L. De Veylder, D. Inzé, D. Weijers, M. J. Bennett, and T. Beeckman, Curr. Biol. **20**, 1697 (2010).
[6] J. Pritchard, A. D. Tomos, and R. G. Wyn Jones, J. Exp. Botany **38**, 948 (1987).
[7] G. T. S. Beemster and T. I. Baskin, Plant Physiol. **116**, 1515 (1998).
[8] M. C. Jarvis and M. C. McCann, Plant Physiol. Biochem. **38**, 1 (2000).
[9] O. Klymenko, J. Wiltowska-Zuber, M. Lekka, and W. M. Kwiatek, Acta Phys. Pol. A **115**, 548 (2009).
[10] N. C. Santos and M. A. R. B. Castanho, Biophys. Chem. **107**, 133 (2004).
[11] J. L. Alonso and W. H. Goldmann, Life Sci. **72**, 2553 (2003).
[12] B. Capella and G. Dietler, Surf. Sci. Rep. **34**, 1 (1999).
[13] J. R. Withers and D. E. Aston, Adv. Colloid Interface Sci. **120**, 57 (2006).
[14] E. A. Hassan, W. F. Heinz, M. D. Antonik, N. P. D'Costa, S. Nageswaran, C. A. Schoenenberger, and J. H. Hoh, Biophys. J. **74**, 1564 (1998).
[15] B. J. Briscoe and K. S. Sebastian, Proc. R. Soc. A **452**, 439 (1996).
[16] Y. T. Cheng and C. M. Cheng, Mater. Sci. Eng., R **44**, 91 (2004).
[17] B. J. Briscoe, L. Fiori, and E. Pellilo, J. Phys. D **31**, 2395 (1998).
[18] K. D. Costa and F. C. P. Yin, J. Biomech. Eng. **121**, 462 (1999).
[19] A. E. Pelling and M. A. Horton, Pflügers Archiv Eur. J. Physiol. **456**, 3 (2008).
[20] W. C. Oliver and G. M. Pharr, J. Mater. Res. **7**, 1564 (1992).
[21] A. Bolshakov and G. M. Pharr, [http://www.osti.gov/bridge/purl.cover.jsp].
[22] W. C. Oliver and G. M. Pharr, J. Mater. Res. **19**, 3 (2004).
[23] W. Gindl and T. Schoberl, Composites: Part A **35**, 1345 (2005).
[24] Y. T. Cheng, Z. Li, and C. M. Cheng, Philos. Mag. A **82**, 1821 (2002).
[25] W. Ni, Y-T. Cheng, M. J. Lukitsch, A. M. Weiner, L. C. Lev, and D. S. Grummon, Appl. Phys. Lett. **85**, 4028 (2004).
[26] H. J. Butt, B. Cappella, and M. Kappl, Surf. Sci. Rep. **59**, 1 (2005).
[27] K. E. Bremmell, A. Evans, and C. A. Prestidge, Colloids Surf. B: Biointerfaces **50**, 43 (2006).
[28] D. Scurr (personal communication).
[29] S. Kasas and G. Dietler Pflügers Archiv Eur. J. Physiol. **456**, 13 (2008).
[30] S. N. Shabala and R. R. Lew, Plant Physiol. **129**, 290 (2002).
[31] J. Pritchard, R. G. Wyn Jones, and A. D. Tomos, J. Exp. Botany **41**, 669 (1990).
[32] K. J. Van Vliet, G. Bao, and S. Suresh, Acta Mater. **51**, 5881 (2003).
[33] W. Gindl, H. S. Gupta, T. Schoberl, H. C. Lichtenegger, and P. Fratzl, Appl. Phys. A **79**, 2069 (2004).
[34] B. Brandt, C. Zollfrank, O. Franke, J. Fromm, M. Goken, and K. Durst, Acta Biomaterialia **6**, 4345 (2010).